Analytic hierarchy process applied to landslide susceptibility mapping of the North Branch of Argentino Lake, Argentina

Silvana Moragues, María Gabriela Lenzano, Mario Lanfri, Stella Moreiras, Esteban Lannutti & Luis Lenzano

Natural Hazards

ISSN 0921-030X

Nat Hazards
DOI 10.1007/s11069-020-04343-8

Springer

Natural Hazards
https://doi.org/10.1007/s11069-020-04343-8

ORIGINAL PAPER

Analytic hierarchy process applied to landslide susceptibility mapping of the North Branch of Argentino Lake, Argentina

Silvana Moragues[1] · María Gabriela Lenzano[1] · Mario Lanfri[2] · Stella Moreiras[1] · Esteban Lannutti[1] · Luis Lenzano[1]

Received: 11 April 2019 / Accepted: 25 September 2020

Abstract
In the present study, we achieved the susceptibility mapping to slope instability processes by the implementation of Analytic Hierarchy Process and Weighted Linear Combination methods, in the North Branch of Argentino Lake, Southern Patagonian Icefield. The strong retraction of the glaciers in the area has triggered paraglacial readjustments, producing instability processes that favor the generation of mass removal processes. The results obtained from optical satellite images show that the highest degrees of susceptibility (4 and 5) are located on the western slopes of the Upsala Channel, Bertacchi and Cono Tributary Glaciers, and the Moyano and Norte Valleys, respectively. These slopes coincide with the geographic location of previous events surveyed by the inventory of unstable areas of the zone. Low degrees of susceptibility are found on the downhill valleys, outcrops rock and glaciers. The Consistency Ratio was 0.069, indicating that being less than 0.1 the study is reliable. The study sheds light on the knowledge of slopes and valleys that are more susceptible to processes of instability in mountainous areas, which would make it possible to prevent possible hazards associated with these events.

Keywords Analytic hierarchy process (AHP) · Weighted linear combination (WLC) · Susceptibility mapping · Slope instability process · North Branch of Argentino Lake (SPI)

1 Introduction

A landslide is the movement of a mass of rock, debris, or soil down a slope by the effects of gravity (Cruden 1991). The occurrence of landslides is related to various factors, including climate, hydrology, lithology, structure, and geomorphology. Landslide susceptibility

✉ Silvana Moragues
smoragues@mendoza-conicet.gob.ar

[1] Instituto Argentino de Nivología, Glaciología y Ciencias Ambientales (IANIGLA)-Centro Científico Tecnológico (CCT), CONICET-Avda. Ruiz Leal s/n. Parque General San Martín. CP 5500, Mendoza, Argentina

[2] Consultoría en Alerta y Respuesta Temprana a Emergencias (CAEARTE), Comisión Nacional de Actividades Espaciales (CONAE), Argentina Ruta C45. Km 8. CP 5187 - Falda del Cañete, Córdoba, Argentina

Published online: 13 October 2020

mapping (LSM) is an effective tool for understanding the probability of the spatial distribution of future landslides (Feizizadeh et al. 2014). According to IUGS (1997), adapted by Fell et al. (2008), the determination of landslide susceptibility on a certain area relies on the classification, estimation of the area or volume (magnitude), and the spatial distribution of observed and potential landslides in the surrounding slopes.

Landslide susceptibility map relies on a rather complex knowledge of slope movements and their conditioning factors (Ayalew et al. 2004), and on an inventory map of instable areas. Furthermore, it is necessary to classify the relative stability of the area into categories ranging from stable to unstable. It should be noted that triggering factors are not considered in a susceptibility analysis due to their dynamic character (Suarez 2009) and it is not always possible to include every aspect in a susceptibility analysis (Moreiras 2005). Recently, landslide susceptibility mapping has been made possible due to the accessibility and variety of remote sensing data and thematic layers as conditioning factors data using Geographic Information Systems (GIS) (Scaioni 2013; Qiao et al. 2013). However, given the development of GIS and remote sensing technology, more sophisticated spatial models have been applied to landslide susceptibility mapping (Gorsevski et al. 2006a).

Several different methods and techniques for landslide susceptibility mapping have been proposed or tested. Landslide susceptibility mapping methods can be classified as qualitative or quantitative, and as direct or indirect (Guzzetti et al. 1999). There are mainly four methods available to map landslide susceptibility, namely landslide inventory-based probabilistic, deterministic, heuristic, and statistical techniques. The heuristic approach based on the a priori knowledge of all causes and instability factors involved in the instability of the area under investigation. Thus, it is a mostly qualitative approach that depends on how well and how much the researcher/professional understands the geomorphological processes acting upon the terrain (Guzzetti et al. 1999). This method adds a certain degree of subjectivity to the assignment of weights and their influence on the triggering of landslides based on the criterion of the operator. Therefore, this situation hinders the comparison of results achieved by different authors (Gorsevski et al. 2006b). Heuristic analysis (qualitative approach) is based on the intrinsic abilities of specialists to analyze aerial photographs and satellite images or to conduct field surveying (Yilmaz and Yildirim 2006).

Semi-qualitative methods are qualitative approaches that apply weighting and qualification procedures. The Analytic Hierarchy Process (AHP) by Saaty (1980) and the Weighted Linear Combination (WLC) were first introduced by Voogd (1983), and they belong to qualitative methodologies. AHP is widely used for landslide susceptibility mapping (Barredo et al. 2000; Ayalew et al. 2005; Gorsevski et al. 2006b; Yalcin 2008; Wu and Chen 2009; Kayastha et al. 2012; Shahabi and Hashim 2015), given its easy implementation and sparse use of detailed in situ and laboratory data required. In addition, AHP is a well-known method of the multicriteria technique, which has been incorporated into Geographic Information Systems-based suitability procedures (Jankowski and Richard 1994; Marinoni 2004); while decisions are taken using weighting by relative pairwise comparisons (Saaty 1980). A very important step for the generation of final susceptibility maps is the application of the WLC analytic method. This method allows multiattribute decision-making based on the importance of these criteria where the weights are incorporated to form a single score of evaluation (Gorsevski et al. 2006b). Finally, the Multicriteria Evaluation method (MEM) is applied for the analysis of landslide susceptibility, which allows to evaluate quantitatively the consistency in the assignment of weights, thus lessening the subjectivity factor in the treatment of variables.

One of the main causes for slope instability in deglaciated environments is the loosening of moraine material due to the retraction of glaciers and, therefore, the loss of support as a result

of the paraglacial processes. In this sense, the Southern Patagonian Icefield (SPI), especially the Upsala Glacier, shows instability events given the paraglacial processes occurring in the area (Moragues et al. 2019a, b). Although glacier recession and steep slopes are one of the main causes of instability, there is a combination of conditioning and triggering factors that cause and affect these processes (Moragues et al. 2019b). Hence, the goal of this study is to map the susceptibility to instability processes in the Northern Branch of the Argentino Lake. Analytic Hierarchy Process Method (AHP), Weighted Linear Combination Method (WLC), and Multicriteria Evaluation Method (MEM) were used and combined on SPOT 6–7 optical satellite images data.

The North Branch area of Argentino Lake is an international landscape seeing a destination that attracts many tourists. At least 700.000 tourists sail in boats through the Upsala Channel during the summer season, being exposed to the occurrence of landslide processes (Moragues 2020). Particularly an extraordinary event occurred in February 2013 generating a large tsunami that caused destruction along the coast of the Upsala Channel (Moragues et al. 2019a). Fortunately, this event happened during the night where not bouts were sailing on the North Branch Lake. However, the instability processes could generate potential risks for tourist activities. In the area there is a wide spectrum of glaciological research (e.g., Skvarca et al. 1995; Sakakibara et al. 2013; Moragues et al. 2018; Foresta et al. 2018); however, there is a deficiency of studies dedicated to the susceptibility and risk for these processes. Therefore, the elaboration of a landslide susceptibility map provides new and relevant contributions to the knowledge and understanding of the paraglacial processes that occur on the slopes of the Upsala Channel and surrounding valleys. In this way, decisions can be made on land use plans for the reduction, prevention, and/or mitigation of the possible hazard of the area associated with these events.

1.1 Study area

The study area is located in the Southern Patagonian Andes, in Santa Cruz province, Argentina. The slopes under study are located in the Southern area of Los Glaciares National Park on the North Branch of the Argentino Lake, Southern Patagonian Icefield (SPI) (Fig. 1). SPI is aligned with the West wind's axis (Naruse and Casassa 1985); its western edge receives heavy rainfalls and snowfalls given the orographic effect, with an estimated average annual range of 6400 mm (Garreaud et al. 2013). The mean annual temperature is 6 °C approx. (Carrasco et al. 2002), which makes it possible for the Nothofagus native forest to coexist together to the ice located on the periphery of the glaciers front.

The area presents a geological context characterized by the presence of a volcanic-sedimentary complex corresponding to the Austral Basin (Kraemer and Riccardi 1997). The morphometry of the current Upsala Channel was mainly formed by the erosive work formerly caused by the large Upsala Glacier, which developed toward the Andean foreland area over weak lithologies such as the slate rocks prevailing in the area (Lo Vecchio et al. 2016).

2 Data used

2.1 Optical satellite images

SPOT (Satellite Pourl' Observation de la Terre) 6 and 7 images were used with an L2A processing level and 1.5 m spatial resolution (https://catalogos.conae.gov.ar/catalogo/catal

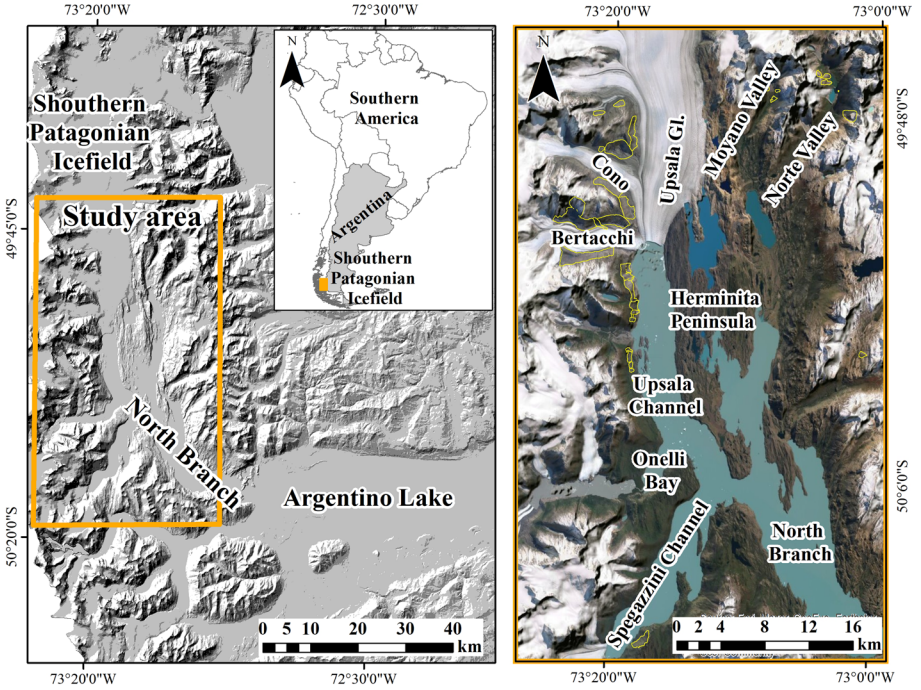

Fig. 1 Study area in the North Branch of Argentino Lake, Southern Patagonian Icefield (SPI), Santa Cruz, Argentina. Areas of slopes instability process (yellow solid line), detected by photointerpretation

ogo.html); Table 1 shows the applied images that cover the study area. To cover the area, four images taken between October and April were chosen, considering the sparse availability of images without cloud cover due to the prevailing climatic conditions (Sagredo and Lowell 2012). The images were used for identifying and mapping the areas of instability by photointerpretation. As of these images, an inventory was created, and information regarding lithology aspects, distance to geological faults, and geomorphology was collected (Fig. 2).

2.2 Digital elevation model

The Digital Elevation Model (DEM) ALOS PALSAR (Phased Array-type L-band Synthetic Aperture Radar), an RTC (Radiometrically and Terrain Corrected Geocoded GeoTIFF) product, with a resolution of 12.5 m was applied to obtain the morphometric parameters (slope, aspect slope, and plan curvature) (Fig. 2). The DEM was obtained from the Alaska Satellite Facility platform (https://www.asf.alaska.edu/sar-data/palsar/).

2.3 General settings

All input spatial data variables, intermediate and final susceptibility maps, were projected onto the Datum WGS-84, 18S UTM system using the QGIS 2.18.19 and ENVI 4.8 software, respectively. The factors were homogenized into digital format, converting all the information to a raster format, using the same number of rows (4890) and

Table 1 SPOT satellite images used (www.catalogos.conae.gov.ar/catalogo/catalogo-de imagenes.html)

Scenes ID	Acquisition date mm-dd-yyyy	Sensor	Spatial resolution	Spectral mode
SPOT6_20160130_1414416_PMS_W073S50_L2A_16GT_065×130_32718	01-30-2016	SPOT 6	1, 5 m	Fusion 3 bands (natural color)
SPOT6_20160303_1410356_P_W073S50_L2A_16GT_064×060_4326_PAR	03-03-2016	SPOT 6	1, 5 m	Panchromatic
SPOT6_20161016_1413584_BUNDLE_W073S50_L2A_16JR_049×219_32718	10-16-2016	SPOT 6	1, 5 m + 6 m	Bundle (multispectral and panchromatic)
SPOT7_20170401_1428414_BUNDLE_W073S50_L2A_16JR_071×239_32718	04-01-2017	SPOT 7	1, 5 m + 6 m	Bundle (multispectral and panchromatic)

columns (2810). Thus, the spatial resolution of every product was converted to 12.5 m, taking as a base the size of the DEM pixel. This way, all layers for calculation were integrated correctly in the Geographic Information System (GIS).

3 Cartographic data and thematic maps generation

3.1 Conditioning factors of instability

In order to produce landslide susceptibility maps, it is important to know the intervening conditioning factors and to prepare all necessary thematic maps (Ahmed 2015). Conditioning (quasi-static) factors contribute to susceptibility and relate inner properties that include geomorphological and geological characteristics, slope gradient, slope aspect, elevation, geotechnical properties, long-term drainage patterns, and vegetation cover (e.g., Dai and Lei 2001; Cubito et al. 2005; Moreiras 2005; Kawabata and Bandibas 2009). The combination and multiplicity of data for the study of landslides optimize the techniques and its derivate results. For generating the susceptibility zoning, a certain number of conditioning factors were selected, and are detailed below.

3.1.1 Slope angle

Most of the studies about susceptibility due to mass movements use the slope angle as one of the most important independent variables (e.g., Brabb et al. 1972; Corominas et al. 2003; Guzzetti et al. 2006; Moreiras 2005, 2009; Marta et al. 2010; Kayastha et al. 2013). The critical inclination angle in mountain areas for mass removal is 30°–32° (Clarke and Burbank 2010; Tofelde et al. 2017), although slopes with lower angles can become unstable. According to Varnes (1984), in order to generate the slope map, the slope angle was divided into six classes: steep (> 70º), very strong (50°–70°), strong (30°–50°), moderate (15°–30°), gentle (5°–15°), and flat (0°–5°).

3.1.2 Geomorphology

We considered in this variable seven classes involving geomorphological processes and deposits: lateral moraine, terminal moraine, glacier-fluvial plain, glacier, water bodies validated according to Glasser et al. (2008) and Moragues et al. (2019b), and, furthermore, the classes outcrop rock and undefined landform were added based on the classification made by Lo Vecchio et al. (2016). Those slopes currently uncovered by ice were considered. On the other hand, water bodies were not taken into consideration for the analysis as they are lake beds resulting from glacial erosion that may produce underwater landslides (Beigh et al. 2019). However, the North Branch area of Argentino Lake lacks on studies and knowledge of underwater mass removal processes. The category undefined landform was used when the surface of deposits or landforms were not distinguished by remote sensing due to dense vegetation even the slope stability behavior of this class is uncertain. Previous landslide of considerable magnitude was generated lateral moraines covered by vegetation (Moragues 2020).

3.1.3 Aspect slope

The orientation of a given slope is an important factor for instability since it is related to a greater or lower amount of incoming solar radiation. In this study, slope aspect was divided into six classes according to the orientation of the chosen slopes: *Sunny slope*: North (0°–22.5°/337.5°–360°), Northeast (22.5°–67.5°), East (67.5°–112.5°), West (247.5°–292.5°), and Northwest (292.5°–247.5°); *Shaded slopes*: South (157.5°–202.5°), Southeast (112.5°–157.5°), Southwest (202.5°–247.5°), and flat (0°). It should be clarified that the sixth class of the aspect slope results from the joint of the shaded slopes that are exposed to less sunshine. Therefore, they are not as prone to generate processes of instability.

3.1.4 Lithology

The physical properties and the resistance of each material from a certain lithological type determine its tense deformation behavior, and, as a result, its stability (Moreiras 2009). For this variable, information concerning the lithology map generated by Moragues et al. (2019b) was used. The weight values were assigned for generating the lithology map according to the resistance of the rocks composing each lithological formation. In this sense, the glacier-covered area and the water bodies were codified with a 0, since the lithology under them is unknown. Hence, only the outcrop lithological formations (four classes) were considered according to the geological formations and characteristics (Kraemer and Riccardi 1997; Lo Vecchio et al. 2016) (Fig. 2).

1. *El Quemado complex* pyroclastic rocks composed of andesites, dacites, and rhyodacites. Volcanic rocks in the area are characterized by north–south, westwards dipping cleavage fracture. Outcrops are characterized by tight folding associated with inverse faulting. This allows for the exposure of interdigitating massive psefites and pyroclastic rocks of this complex west of Rio Mayer.
2. *Río Mayer formation* prevailing of slate rocks, initially laminated dark gray or black pellets that are fissile. In the lower levels most sections, with fracture and interdigitating with calcareous levels up to 4 cm thick, with red alteration colors and positive relief.
3. *Bahía La Lancha formation* this is identified by two well-defined lithological types: (1) it is characterized by its sedimentary aspect, and it is constituted by an alternation of sandstone and pellets with a granulometry that varies from thick conglomerate sandstone to fine sandstone of light gray or brown color; (2) Green to gray phyllites showing progressive loss of sedimentary features, appearance of foliation planes with a satin sheen and green to gray tones.
4. *Cerro Toro formation* slate formation; dark gray, massive pellets, with an alternation of greenish-gray sandstones. This unit is recognizable by its dark gray tones and a typical alternating hard-soft erosion profile.

3.1.5 Plan curvature

There are two types of plan curvature which determines either flux convergence (concave) or divergence (convex). There is also the profile curvature, which is parallel to the slope and indicates the direction of the maximum slope. The maximum slope affects the acceleration

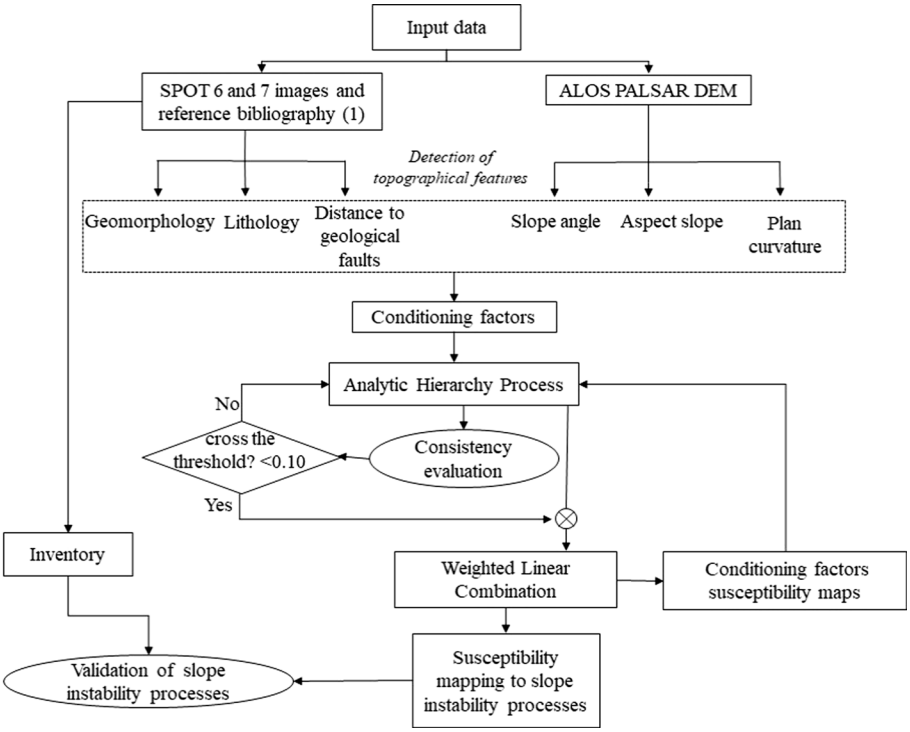

Fig. 2 Workflow for mapping susceptibility to slope instability processes. Note that the detection of topographical features was done on the basis of photointerpretation and the background studies: Kraemer y Riccardi (1997), Glasser et al. (2009), Ghiglione et al. (2009), Lo Vecchio et al. (2016), and Moragues et al. (2019b)

or deceleration of the currents on the surface (Felicisimo 1994). Plan curvature was applied in this study, since it influences the slope instability processes according to the convergence or divergence of water during the passing of flux down the slope (Ercanoglu and Gokceoglu 2002). For this reason, this parameter constitutes one of the conditioning factors controlling landslide occurrence (Nefeslioglu et al. 2008). This variable was divided into three classes: concave (< -0.001), convex (> 0.001), and flat ((-0.001)–0.001).

3.1.6 Distance to geological faults

Faults create a gap between two distinctive lithological units and generate fractures and joints within the lithological unit that can propagate landslide activity (Regmi et al. 2016). Active faults increase susceptibility to these processes since the rocks near a fault are weaker due to the vibration wave that occurs over time (Leir et al. 2004). In the study area, the location of reverse faults was obtained from Kraemer and Riccardi (1997) and Ghiglione et al. (2009). The Andean region includes the folded strip and internal route at an altitude of approximately 3000 m A.S.L. in its western edge, and it is partially covered by glaciers. To the west, the structural relief decreases toward the depression of the Upsala Glacier where Cretaceous rocks overlying the Palaeozoic base emerge (Ghiglione et al. 2009). The geological formations that affect the area's faults are El Quemado Complex,

Mayer River, and La Lancha Bay (Kraemer and Riccardi 1997; Ghiglione et al. 2009). Multiple buffers were generated to estimate the impact area over the lithology, considering the that the proximity of these formations to the faults (up to 1000 m) increases the susceptibility of the material. Based on this fact, four classes were generated: 0–200 m, 200–500 m, 500–800 m, 800–1000 m.

3.2 Inventory: areas with slopes instability processes

Accurate and reliable landslide inventory data are crucial for landslide susceptibility mapping (Corominas et al. 2014; Zhu et al. 2014). Landslide inventory maps show locations and features of landslides that have occurred in the past. Although they usually do not show the mechanism(s) that triggered them (Shahabi and Hashim 2015). Therefore, inventory maps provide useful information about the spatial distribution of locations of existing landslides and the potential occurrence (Razak et al. 2013). Hence, the slopes instability geoforms were detected by optical satellite images photointerpretation, while some geoforms were verified in the field.

4 Methodology

In the first stage, the thematic maps of the six conditioning factors of the area were generated based on satellite images and DEMs (Fig. 2). Then, the heuristic method (AHP and WLC) was applied to determine the relative importance of the factors and their classes concerning susceptibility. From the consistency index, the right assignment of weights as a weighting mechanism for each factor and their respective classes was evaluated for the construction of every factor maps. Finally, the Easy-AHP v1.0 plugin (analyses AHP and WLC) in QGIS was applied to obtain the final susceptibility to the instability processes of the area in the North Branch of the Argentino Lake. These results are validated with the generated inventory map. Figure 2 shows the overall processes proposed.

4.1 Analytic hierarchy process (AHP)

The AHP method is a common tool for analysing complicated spatial problems focusing on site selection, urban planning, and natural hazard susceptibility analysis (Suarez 2009). It is a semi-quantitative method in which decisions are taken applying weightings through relative pairwise comparisons, with inconsistencies in the decision-making process (Saaty 1980). This method consists of three principles, which, in general terms guide the evaluation process: the construction of hierarchies, the setting of priorities, and an evaluation carried out by means of a logic consistency index. The processes involve the following five steps: (1) division of the component problems precision; (2) disposition of these factors on a hierarchic order; (3) assignment of numeric values, to determine the relative importance of each factor according to its subjective relevance; (4) configuration of a comparison matrix; and (5) calculation of the normalized main eigenvector, that provides the weight factor up to the moment (Saaty and Vargas 2001). According to Thanth and De Smedt (2012), the advantages of using AHP in a landslide analysis are as follows: (1) all types of information can be included in the discussion process; (2) judgment is structured so that all the information is taken into account; (3) discussion rules can be based on experience; (4) once a consensus is reached, weights for each relevant factor are obtained automatically by eigenvector calculation of the decision matrix;

and (5) inconsistencies in the decision process can be detected and, therefore, corrected. Also, this method is subjective in the ranking of factors and weights of geospatial parameters that determine from one experts' knowledge on the subject and area (Kayastha et al. 2013; Meena et al. 2019).

Based on the data availability of the study area, six conditioning factors and their corresponding classes were selected. A hierarchic order was granted to each factor according to the importance and the affectation to slope instability in the area as well as the weights assignment (level of relative importance). The selection criteria for the weights were relative, depending on each conditioning factor, knowledge of the area, and existing background. The data of factors classes were added (Σxj) ordered in rows and columns to form the overall matrix. To obtain the relative weight of every factor and class, the summation of every row and column is divided($\Sigma(\Sigma xj/n)/(\Sigma xj/n)$), being n the number of factors. The sum of all the weighted weights in the matrix must be 1.

4.1.1 Consistency index evaluation

Consistency ratio (CR) is a non-statistic index that is determined by the quotient between the Consistency Index (CI) and the Random Consistency Index (RI) obtained from Eq. (1). CR evaluates the consistency of the decision-making process of the operator providing the decision judgement (Saaty 2000).

$$\mathrm{CR} = \mathrm{CI}/(\mathrm{RI}) \tag{1}$$

CI is a measure of deviation from the consistency of the pairwise comparison matrix. It is obtained from the following expression: $\mathrm{CI} = \frac{\lambda_{\max} - n}{n-1}$, where $\lambda_{\max}$ is the maximum eigenvalue of the comparison matrix and n is the number of conditioning factors. In some cases, where there may be an inconsistency in the judgments, the eigenvalue tends to be higher than the range of the matrix. The maximum value of the pairwise comparison matrix was obtained by multiplying the values of the comparison matrix (AHP) by the relative weights granted in every row.

RI is the consistency index of a random reciprocal matrix with reciprocals forced, showing values that range from 1 to 9. Saaty (1980) defines this random matrix to give consistency to the given weights of each factor (see Table 2). If CR is lower than 0.1, the consistency of the model is acceptable; if it is higher than 0.1, it will be necessary to recalculate the pairwise comparison (Hung et al. 2016).

4.1.2 Multicriteria evaluation method (MEM)

This method allows to evaluate quantitatively the consistency in the assignment of weights in order to decrease the inherent subjectivity, a factor they have. In this study, MEM is based on analytic hierarchies and linear sums weighted from the factor weights and their classes (Saaty 1980; Eastman et al. 1995). First, to determine the weights,

Table 2 Random consistency index (RI) (Saaty 1980, 2000)

n	1	2	3	4	5	6	7	8	9	10	11	12	13	14	15
RI	0	0	0.58	0.90	1.12	1.24	1.32	1.41	1.45	1.49	1.51	1.53	1.56	1.57	1.59

the priorities of the conditioning factors are settled through the pairwise comparison of elements according to the influence of the slope instability (Hervás et al. 2003). A database was created by selecting and mapping the conditioning factors of instability. Hence, every factor was divided into classes, and weights were assigned to them according to the relative influence on the slope instability processes. It should be noted that in this study, the scale made by Saaty (1980) was adapted to that generated by Roa (2007) for the instability processes (see Table 3).

4.2 Weighted linear combination (WLC)

This method is a hybrid between the quantitative method and the qualitative method (Ayalew et al. 2004), based on the approach of a combination of qualitative maps (heuristic analysis) (Shahabi and Hashim 2015). This is the simplest method that adds criteria to form a single score of evaluation. In the WLC method, each criterion is multiplied by its weight from the pairwise comparison, and the results are summed (Eq. 2):

$$S = \sum_i w_i \mu_i \tag{2}$$

where susceptibility S is the final score, w_i is the weight of the criterion i, and μ_i is the criterion standardized score (Gorsevski et al. 2006a). The decision-making operator directly affects the weights of proportional importance to each thematic layer.

Each factor was multiplied by the assigned weighted weight to obtain a total punctuation for each of them (Feizizadeh and Blaschke 2013), and, lastly, the corresponding results were added to all the factors. Finally, the susceptibility map to slope instability processes was made using the WLC through the combination of all the layers weighted in individual maps (Voogd 1983). Then, a slope failure susceptibility index was obtained by a weighted linear sum (Voogd 1983). With the given results, a whole number was codified to every class, and the total area of the unit and the slipped surface (km^2) of each class of the factor were calculated (Table 6). The obtained ranges were provided by the relative weights considering those of each class. The selected susceptibility degrees were as follows: 1 (very low), 2 (low), 3 (moderate), 4 (high), and 5 (very high). Consequently, the susceptibility category for each class and factor, respectively, was achieved and were included in the final susceptibility map (Marcano et al. 2015).

The final susceptibility map was generated and zoned by the following three steps:

Table 3 Assessment scale to estimate the coefficient to be assigned to each of the variables considered in the matrix of analytical hierarchies according to Roa (2007). *Source* Modified Caaty scale (1977)

Importance level	Definition	Description of criterion *x*, when compared to *j*
1	Equal preference	The two criteria (*x, j*) contribute equally to mass removal processes
2	Moderate preference	Past experiences slightly favor criterion (*x*) over (*j*)
3	Strong preference	Practically the dominance of criterion (*x*) over (*j*) is demonstrated
4	Absolute preference	There is evidence that determines the supremacy of criterion (*x*)

1. The input parameters, meaning the susceptibility maps for factors in relative order were selected, from the most instable variable to the most stable variable.
2. The weight values in the comparison matrix of each row were completed. In this step, the CR, CI, and RI were automatically calculated.
3. The Weighted Linear Combination (WLC) was calculated generating a table with the weighting values assigned to the factors composing the matrix. The WLC procedure is carried out through the following formula (Eq. 3) (Palma Herrera 2015):

$$\mathrm{WLC} = (S * \mathrm{Ww}) + (G * \mathrm{Ww}) + (A * \mathrm{Ww}) + (L * \mathrm{Ww}) + (C * \mathrm{Ww}) + (F * \mathrm{Ww}) \quad (3)$$

where *S*, *G*, *A*, *L*, *C*, and F are the initials that stand for the conditioning factors of slope instability (slope, geomorphology, aspect slope, lithology, plan curvature, distance to geological faults), *y Ww* (weighted weight).

Therefore, the final susceptibility map was validated by the inventory map. This simple type of validation based on spatial cross-checking of the mapping results serves as a first indicator for the plausibility of the landslide susceptibility map (Hung et al. 2016).

5 Results

5.1 Susceptibility by conditioning factors

The incidence and relative weight of the six conditioning factors in the slopes instability were carried out based on the selection and analysis of their classes in the area of the North Branch of the Argentino Lake (Fig. 3). The results of the AHP generated a matrix where the weighted weights were settled for all the classes of every factor (see Table 4), and which served as a base for producing the susceptibility maps for each factor.

Afterward, each factor influencing slope instability is analyzed.

- *Slope angle* The moderate type slopes (30°–50°) and the strong slopes (30°–50°) (Fig. 3a) prevail in the area, with relative weights of 0.17 and 0.13, respectively (Table 4). These slopes are composed of rocky outcrops as is the case of Herminita Peninsula. The classes with higher relative weight correspond to steep (>70°), very strong (50°–70°), and strong (30°–50°) that cover 18% of the total surface under study (2,644 km^2), and they are located on the higher slopes (Fig. 3a). The last three classes represent the areas with a greater slipped surface (24.08 km^2) (Table 5) and with high and very high susceptibility degrees (4 and 5) (Fig. 4a). Furthermore, the glaciers with flat slopes (<5°) show faint possibilities of causing instability.
- *Geomorphology* Seven classes were represented (Fig. 3b); the classes with the highest relative weight for instability process are the lateral and terminal moraine, and undefined landform present in the area (Table 4). The lateral moraine class has the highest weight (0.25) with a susceptibility degree of 5 (very high), representing 1.46% of the total km^2, being the slipped area of 26.66 km^2 (Table 5). The terminal moraine and undefined landform classes have a susceptibility degree of 4 (high). Of the total area of the undefined landform class (399.53 km^2), 4.97 km^2 correspond to a slipped surface; this class and the lateral moraine, are the only ones that show instability processes. The classes that show lower susceptibility and lower relative weight are the glacier-fluvial plain (0.07), and outcrop rock (0.04), with a low and very low degree of susceptibility

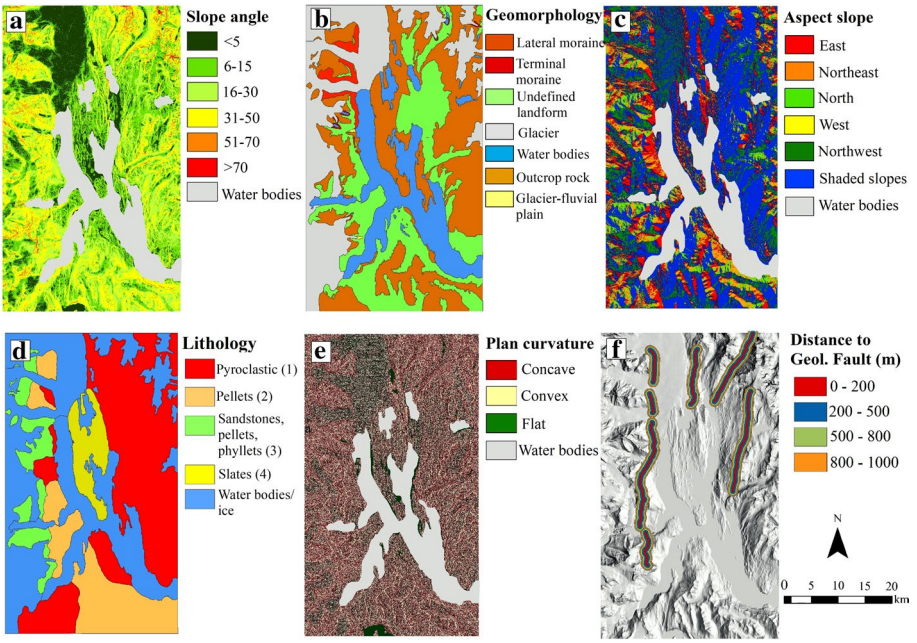

Fig. 3 Conditioning factors of instability with their respective classes in the area of study. **d** Geological Formations: (1) El Quemado Complex (pyroclastic: andesites, dacites, riodacites), (2) Río Mayer (Cretaceous pellets), (3) Bahía La Lancha (sandstones, pellets, phyllites), and (4) Cerro El Toro (slates: pellets, sandstones)

(Table 5). This is can be explained due they are plain covers and rocky that present a faint possibility of generating instability processes (Fig. 3b).

- *Aspect slope* The slopes that are more exposed to sunlight have a higher relative weight on instability processes (Fig. 3c, Table 5). In the area, these are the slopes oriented toward the East (0.27), Northeast (0.26), and North (0.21), with a high (4) and very high (5) degree of susceptibility (Fig. 4c). Then, of the total area corresponding to slope orientation (2,645.26 km^2), these three classes represent 42%, and have 18.21 km^2 of slipped area. On the contrary, the slopes orientated toward the West and the Northwest, and the shaded slopes (Fig. 3c) show lower relative weight values for instability 0.12, 0.10, and 0.04, respectively. They represent 1533.75 km^2 of the total as the class covers, with 30% of the slipped area (Table 5), with a low and very low susceptibility (Fig. 4).
- *Lithology* Lithological formation El Quemado Complex prevails in the area (Fig. 3d), covering the largest area of all the classes (848.31 km^2) formed over pyroclastic rocks (andesites, dacites, and riodacites). This shows the largest amount of geoforms due to instability (15.41 km^2), with the highest relative weight in this factor (0.41) and a very high susceptibility degree (Fig. 4d). The Cretaceous Pellets (Rio Mayer Formation) show a relative weight of 0.35 and high susceptibility. Thus, Rio Mayer and El Quemado Complex have the highest amount of slipped material in the area, 15.41 km^2 and 12.02 km^2, respectively (Table 6). Oppositely, the two other classes have lower relative weights on the instability processes with 0.16 the sandstones, pellets, and phyllites

Table 4 Weighting matrix of the classes of each conditioning factor

Classes of each factor	Weighting matrix in pairs							Peso relativo $\Sigma \frac{\frac{\Sigma ij}{n}}{\frac{\Sigma ij}{n}}$
	1	2	3	4	5	6	7	
Slope angle								
1. Steep (> 70º)	1	3	3	4	4	4		0.33
2. Very strong (50°–70°)	0.33	1	2	3	4	4		0.25
3. Strong (30°–50°)	0.33	0.50	1	2	3	3		0.17
4. Moderate (15°–30°)	0.25	0.33	0.50	1	2	3		0.13
5. Gentle (5°–15°)	0.25	0.25	0.33	0.50	1	2		0.07
6. Flat (0°–5°)	0.25	0.25	0.33	0.33	0.50	1		0.05
Geomorphology								
1. Lateral moraine	1	2	2	3	4	4	4	0.25
2. Undefined landform	0.50	1	2	3	4	4	4	0.23
3. Terminal moraine	0.50	0.50	1	3	4	4	4	0.21
4. Glacier	0.33	0.33	0.33	1	3	3	4	0.15
5. Glacier-fluvial plain	0.25	0.25	0.25	0.33	1	2	2	0.07
6. Outcrop rock	0.25	0.25	0.25	0.25	0.50	0.50	1	0.04
Aspect slope								
1. East (67.5°–112.5°)	1	2	2	3	3	4		0.27
2. Northeast (22.5°–67.5°)	0.50	1	2	3	4	4		0.26
3. North (0°–22.5°/337.5°–360°)	0.50	0.50	1	3	3	4		0.21
4. West (247.5°–292.5°)	0.33	0.33	0.33	1	2	3		0.12
5. Northwest (292.5°–247.5°)	0.33	0.25	0.33	0.50	1	3		0.10
6. Shaded slopes: South (157.5°–202.5°), Southeast (112.5°–157.5°), Southwest (202.5°–247.5°), Flat (0°)	0.25	0.25	0.25	0.33	0.33	1		0.04
Lithology								
1. El Quemado Complex (pyroclastics: andesites, dacites, riodactytes)	1	2	3	4				0.41
2. Río Mayer Fm. (cretaceous pellets)	0.50	1	3	4				0.35

Table 4 (continued)

Classes of each factor	Weighting matrix in pairs							Peso relativo
	1	2	3	4	5	6	7	$\Sigma \frac{\frac{\Sigma ij}{n}}{\frac{\Sigma ij}{n}}$
3. Bahía La Lancha Fm. (sandstones, pellets, phyllets)	0.33	0.33	1	2				0.16
4. Cerro Toro Fm. (slates: pellets, sandstone)	0.25	0.25	0.50	1				0.08
Plan Curvature								
1. Concave (< −0.001)	1	3	4					0.61
2. Convex (> 0.001)	0.33	1	2					0.25
3. Flat ((−0.001)–0.001)	0.25	0.50	1					0.13
Distance to Geological faults								
1. 0–200 m	1	2	2	3				0.37
2. 200–500 m	0.50	1	2	3				0.30
3. 500–800 m	0.50	0.33	1	3				0.23
4. 500–1000 m	0.33	0.33	0.33	1				0.09

Table 5 Statistics of the weight of the values of the classes and category of susceptibility to slope instability

Code	Classes	Area (km2)	Slide area (km2)	Class weight (%)	Degree of susceptibility
1	Steep (> 70°)	14.06	4.59	32.65	5
2	Very strong (50°–70°)	59.21	10.08	17.02	4
3	Strong (30°–50°)	379.87	9.41	2.48	4
4	Moderate (15°–30°)	625.99	6.99	1.12	3
5	Gentle (5°–15°)	513.14	0.62	0.12	2
6	Flat (0°–5°)	1,051.97	0	0	1
Total		2,644.27	31.69	53.39	
1	Lateral moraine	39.0	26.66	68.36	5
2	Undefined landform	399.53	4.97	1.24	4
3	Terminal moraine	4.86	0	0	4
4	Glacier	1,272.51	0	0	3
5	Glacier-fluvial plain	2.14	0	0	2
6	Water bodies	335.76	0	0	1
7	Outcrop rock	624.93	0	0	1
Total		2678.73	31.63	69.6	
1	East (67.5°–112.5°)	281.59	5.60	1.99	5
2	Northeast (22.5°–67.5°)	202.50	5.46	2.69	5
3	North (0°–22.5°/337.5°–360°)	627.18	7.15	1.14	4
4	South (157.5°–202.5°)	234.25	3.39	2.30	3
5	Southeast (112.5°–157.5°),	283.02	3.79	2.04	2
6	Shaded slopes: Southwest (202.5°–247.5°), West (247.5°–292.5°), Northwest (292.5°–247.5°), Flat (0°)	1016.48	2.33	0.23	1
Total		2,645.26	31.72	10.39	
1	Pyroclastics: El quemado complex	848.31	15.41	1.81	5
2	Pellets: Río Mayer Fm	278.35	12.02	4.31	4

Table 5 (continued)

Code	Classes	Area (km2)	Slide area (km2)	Class weight (%)	Degree of susceptibility
3	Sandstones, pellets, phyllites: Bahía La Lancha Fm	143.15	4.53	3.16	2
4	Slates: Cerro Toro Fm	113.87	0	0	1
Total		1383.68	31.95	19.67	
1	Concave (< −0.001)	549.78	–	–	5
2	Convex (> 0.001)	1545.43	–	–	2
3	Flat ((−0.001)–0.001)	549.78	–	–	1
Total		2644.99	–	–	
1	0–200 m	36.40	3.78	10.38	4
2	200–500 m	57.79	6.34	10.97	3
3	500–800 m	61.64	2.94	4.77	3
4	500–1000 m	42.95	0	0	1
Total		198.78	13.06	26.12	

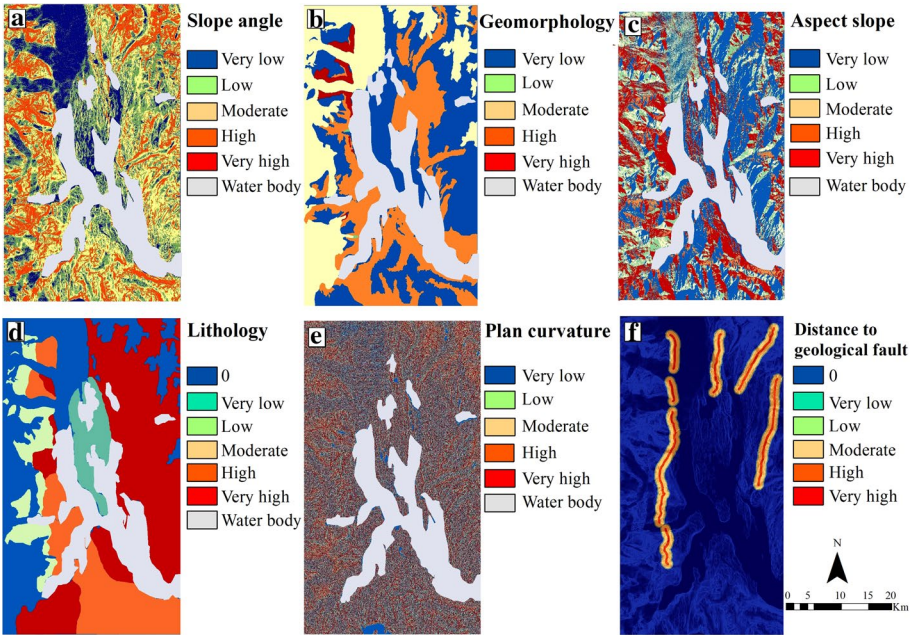

Fig. 4 Susceptibility maps to slope instability processes according to conditioning factors, through the implementation of analytic hierarchy process (AHP) of the area North Branch of Argentino Lake

(Bahía La Lancha Formation) and 0.08 the slates (pellets and sandstone-Cerro Toro Formation) (Fig. 3d, Table 4). The zones cover 18.5% of the area with susceptibility degrees of 2 (low) and 1 (very low) (Fig. 4d), noting that there are instability processes only in Bahía La Lancha Formation (4.53 km^2) (Table 6). Cerro Toro Formation is a big rocky formation of low altitude (200–300 m ASL) (Moragues et al. 2019b) without slipped area (Table 6).

- *Plan Curvature* The concave slopes where fluxes converge (Fig. 3e) have the highest relative weight of the curvature plan factor in the area with a value of 0.61 (Table 4), and a very high susceptibility to instability processes (Fig. 4e). Differently, in convex slopes where fluxes diverge, instability processes have a lower relative weight (0.25) and a low susceptibility degree of 2 (Fig. 4e, Table 5). Finally, the flat terrains located

Table 6 Consistency index for the mapping of susceptibility to processes of slope instability

	Conditioning factors					
	Slope	Geomorphology	Aspect slope	Lithology	Plan curvature	Distance to geological faults
n	6	7	6	6	3	4
λ_{max}	6.61	7.88	6.34	4.18	3	4.09
CI	0.12	0.15	0.07	0.06	0	0.03
RI	1.24	1.31	1.24	0.90	0.58	0.90
CR	0.09	0.09	0.05	0.06	0	0.03

in some valleys and glaciers (Fig. 3e) have a lower relative weight and a very low susceptibility degree of instability processes (Fig. 4e).

- *Distance to geological faults* The faults are located over Moyano and Norte Valleys, and the western side of the Upsala Channel heading N-S and diving west (Fig. 3f). The affectation areas of these faults show that the first distance of 0–200 m (0.37 weight) has a high degree (4) of susceptibility (Fig. 4f), being this zone the most affected area in the event of an earthquake. The area located between the 200–500 m has a relative weight of 0.30 and it shows the largest amount of slipped area with 6.34 km^2 of a total of 13.06 km^2 (Table 5). Also, the area placed in the attitudinal range of 500–800 m (0.23 relative weight) has a moderate susceptibility degree (3) to instability processes similar to the previous one (Fig. 4f). The furthest areas from the faults (800–1000 m) show a relative weight of 0.09, without slipped material, and have a susceptibility degree of 1 (Fig. 4f).

Table 6 shows the order of the conditioning factors for instability in the area with their respective n, λ_{max} IC, RI, and RC. Plan curvature, distance to geological faults, and aspect slope are the factors that show a lower and more reliable Consistency Ratio. The other factors (slope angle, geomorphology, and lithology) show CR values lower than 0.1, which indicates that the weights of all factor classes are accepted.

5.2 Landslide susceptibility mapping

The results obtained in the WLC (Easy-AHP) process about the incidence of the conditioning factors are shown in Table 6. Slope angle factor has the highest relative weight (0.29), which shows that those factors related to topographic and geomorphologic aspects have more incidence on slope instability (see Table 7). The faults show the lowest rank of incidence (0.06). The resulting CR for the final susceptibility map equals 0.069, 6.427 $\lambda_{max,}$ and the CI equals 0.085.

In the final susceptibility map for instability processes in the area (Fig. 5), the largest areas correspond to degrees 1 (very low), 2 (low), and 3 (moderate). Meanwhile, the areas classified with degrees 4 (high) and 5 (very high) are smaller, but still important. The location of the areas showing instability processes coincides with the susceptibility areas with high and very high degrees. Susceptibility degree 5 (very high) can be found on the

Table 7 Weighting matrix of the conditioning factors with their respective classes and the weighted linear combination (WLC) calculated for each factor by Easy-AHP, QGIS

Conditioning factors	Weighting matrix in pairs						WLC
	1	2	3	4	5	6	
1. Slope angle	1	2	2	2	3	3	0.29
2. Geomorphology	0.50	1	2	2	3	3	0.23
3. Aspect slope	0.50	0.50	1	3	2	4	0.20
4. Lithology	0.50	0.50	0.33	1	3	2	0.13
5. Plan curvature	0.33	0.33	0.50	0.33	1	3	0.09
6. Distance to geological faults	0.33	0.33	0.25	0.50	0.33	1	0.06

western slope of the Upsala Channel, near the front of the homonymous glacier, oriented from the northeast to the west where frontal moraines rest. The slopes of the Bertacchi and Cono Tributary Glaciers, as well as the slopes of Moyano and Norte Valleys, reach values up to 4.68, which means that they have a very high susceptibility degree (5). It should be noted that in these slopes the conditioning factors contribute to increasing instability: steep slopes, sunny side slopes, presence of geoforms and loose moraine material, low-resistance lithology, concave curvature, and closeness to geological faults. The areas with a low degree of susceptibility (1–2) are located over glaciers and at Herminita Peninsula,

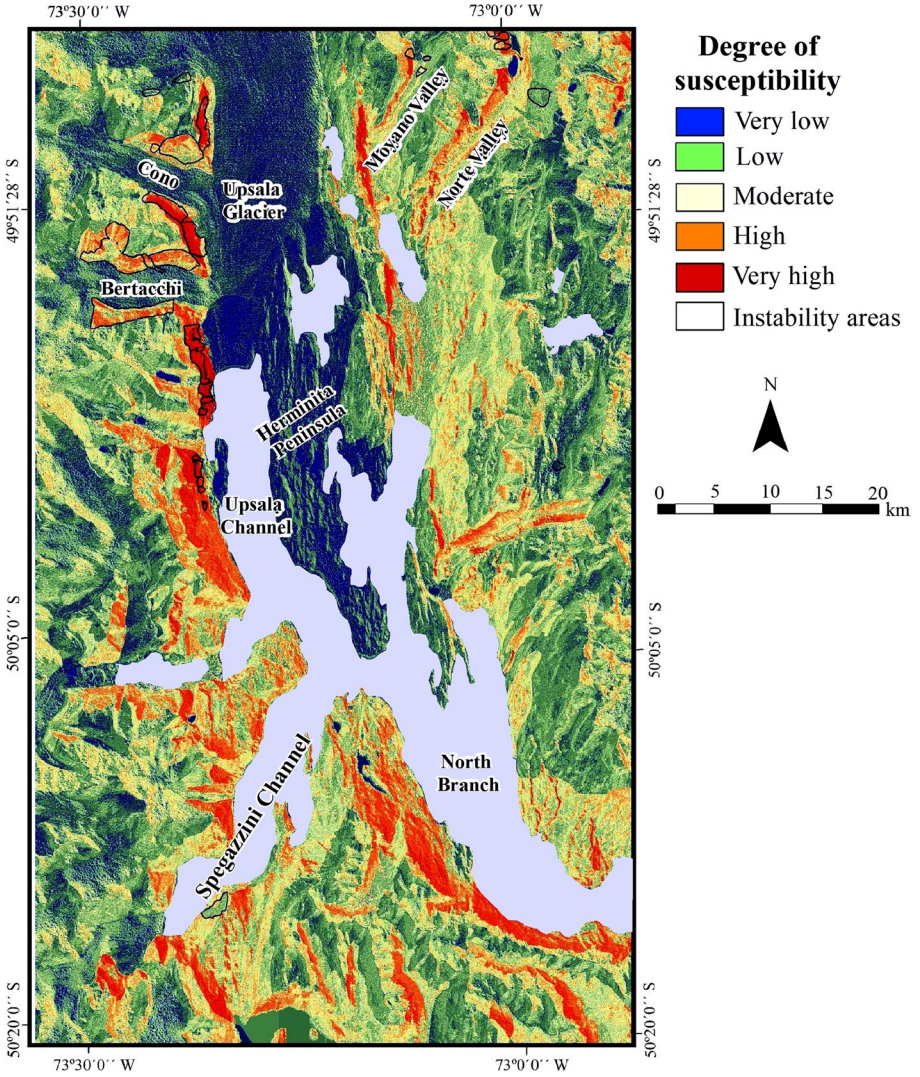

Fig. 5 Susceptibility mapping to the slope instability processes through the implementation of analytic hierarchy process (AHP) and weighted linear combination (WLC), North Branch of the Argentino Lake (Patagonia, Argentina)

the eastern slope of the Upsala Channel, given its rocky formation that is not fissile, and its slope that does not exceed 250–300 m ASL.

From the comparison of the results obtained by the inventory map, it is observed that 32 instability events (paraglacial geoforms) have been recorded and they coincide with the highest susceptibility degrees (see Fig. 5). Moreover, 46.9% (15 events) of the 32 paraglacial geoforms correspond to high and very high susceptibility, 31.2% (10 events) correspond to a moderate degree, and 21.9% of the instability events (7) are located on slopes with low and very low susceptibility.

6 Discussion

Traditionally, conditioning factors, such as those applied herein, have been used for landslide susceptibility map modelling in mountain areas (e.g., Ayalew et al. 2004; Pourghasemi et al. 2012; Chen et al. 2017; Yan et al. 2018; Meena et al. 2019). Nevertheless, there are certain dynamic factors that may trigger instability processes, e.g., land use, dams, road construction, and rainfall, among others (e.g., Hervás et al. 2003; Mondal and Maití 2012; Hasekiogluları and Ercanoglu 2012; Ahmed 2015; Marcano et al. 2015). These factors were not included since the area is located in a natural environment, free of anthropic infrastructure. The extreme meteorological events and earthquakes might be preponderant triggers factors; however, the area lacks local weather and seismic stations for continuous monitoring. On the Chilean side, there are two closest meteorological stations to the area, Torres del Paine at 130 km south of the area, and the O'Higgins station, 180 km north. On the other side, the seismic events can be obtained from worldwide catalogs that locate events; thus, there is no guarantee that they will register earthquakes with local characteristics that could trigger instability processes in the North Branch area. Hence, the election of the applied factors was based on the availability of data in the study area. The factors used in the study can be applied to other areas with similar conditions to assess future comprehensive landslide hazard mitigation measures (Yoshimatsu and Abe 2006). According to Meena et al. (2019) in the Himalayas area, the two conditioning factors that influence the instability processes are the lithology and slope aspect. Contrasting for this study, the slope and geomorphology are the most important variables for susceptibility assessment.

Lithology was not so important due to the particular type of landslides generated from glacial deposits in the study area. Slope instability in this glacial environment seems to be more related to unconsolidated deposits than to outcroppings. According to this landform analysis is fundamental to understand the slope dynamics related to paraglacial processes in a glacial environment where incoherent glacial deposits are the most unstable units. For this reason, this analysis throws that lateral moraine (geomorphology variable) has a higher weight (0.29) compared with the susceptibility of the El Quemado Complex, the main lithology of the region (0.13) (Tables 5 and 7). Moreover, those areas mapped as undefined landforms when they are covered by vegetation correspond to glacial deposits showing high instability processes even they were initially precluded to have undetermined behavior.

Two different scenarios show the highest susceptibility areas in the North Branch (Fig. 5). For the northern areas closer to glaciers of the Upsala Channel, unstable hillslopes are directly related to steep lateral moraines under a factor combination favoring instability (Moragues et al. 2019b). The major number of landslides is concentrated in these areas. Further, in the Southern region, those areas with higher and high susceptibility do not

present instability processes, except for a little landslide in the Spegazzini Glacier (Fig. 5), resulting from the high weight assigned to the highest slopes. This region shows steep relief with sun-exposed hillslopes, but glacial deposit does not predominate (lateral moraine). So even susceptibility degrees of 4 and 5 are detected on a great part of the hillslope of the Western Upsala Channel, they correspond to two completely different environments.

Thus, the main limitation of this heuristic method is the subjectivity in the factor classification and weight assignment that could differ from one expert to another (Saaty 2008; Kayastha et al. 2013). However, the how-known of the environment the weight assessment to the geomorphology, slope angle, and lithology variables resulted in accurate landslide susceptibility for the study area.

On the other side, the material type (e.g., soils, soft rock, or brittle rock) and slope geometry also influence the type of landslide that may be expected (e.g., soil flow, slump, rock avalanche). Also, the knowledge of these parameters can also be used to help predict the type of landslides expected (Gerrard 1994; Cruden and Martin 2013; McColl 2015). However, in the current investigation, no classification of factors was made for the generation of the different types of slides. Instead, all paraglacial geoforms were generalized as instability processes, and this inventory was used to validate the susceptibility map.

The AHP method has been widely used as a decision analysis technique for evaluating the relative importance of the activities related to slope instability in many countries (Ladas et al. 2007; Hung et al. 2016). The combination of the AHP and WLC methods is appropriate for landslide susceptibility mapping in broad mountain areas that show limited input data (Shahabi and Hashim 2015; Hung et al. 2016; Basu and Pal 2017; Rahim et al. 2018). As already mentioned, the selection and weighting of the weights for instability conditioning factors are the most subjective concepts in the study. For this reason, the implementation of the Consistency Ratio (CR) is of utmost importance for determining the consistency in the decision-making process (Kayastha et al. 2013). The results of CR reached 0.069, which indicates that given its value lower than 0.1 the study is reliable. There are studies with different geomorphological characteristics as shown by Ayalew et al. (2004), in the Tsugawa area in the Agana river, Japan; however, they apply similar conditioning factors to the present study, giving a CR of 0.07. There are lower and more consistent CR values in other areas where the combination of the studied factors varies, such as in Western Chipre in the Mediterranean Region, with a CR of 0.00254 (Myronidis et al. 2016). In Tirajana Depression, Gran Canaria Island, the CR value was equal to 0.02, indicating a coherent comparison factor for the area (Hervás et al. 2003). Another susceptibility study was conducted in the Kullu Valley, High Himalayas, India, in which the RC for the AHP method was 0.016 (Meena et al. 2019). Finally, in the case presented by Hasekiogulları and Ercanoglu (2012) in the western region of the Black Sea in Turkey, 11 factors were applied, of which four had to be deleted since they provided a CR higher than 0.1; only those factors lower than that value, with a CR of 0.0797, were used.

From the combination of the AHP and WLC methods, it is shown that the highest degree of susceptibility in the area (4) is located on the slopes to the west of the Upsala Channel, the slopes of Bertacchi and Cono Tributary Glaciers, and the slopes of Moyano and Norte Valleys. These slopes have not been alien to the changes caused by the recession of glaciers, and have suffered instability process during the last years. As a result, it can be noted that the slope located to the west of the Upsala Channel, between the front of the Upsala Channel and Las Vacas Valley shows more susceptibility, reaching values up to 4.68, which means it is close to susceptibility degree 5. For example, the origin of the proglacial lakes in the superior areas of the slopes is related to the water supply generated by the melting of snow during the summer, which may infiltrate and go through the slopes

generating water surges from the higher area to the lake, increasing the possibilities of instability conditions in the area. This is the case of the proglacial Agassiz lagoon, located on the highest area of the western slope and at the foot of Mc Andrews Peak (2613 m ASL), generating a significant contribution of superficial water and underground water to the Agassiz landslide, that occurred in February 2013 (Moragues 2020).

7 Conclusion

The North Branch of the Argentino Lake is a geographical area where two dynamic environments coexist: glacial and paraglacial. The recession of ice masses in these valleys has left slopes exposed to several paraglacial readjustment processes. This is a complex behavior phenomenon, since it depends on the combination of various interrelated factors (conditioning and triggering factors) propitious for the generation of instability. The six conditioning factors for slope instability that were selected are as follows: (1) slope angle, (2) geomorphology, (3) aspect slope, (4) lithology, (5) plan curvature, and (6) distance to geological faults, which provided the necessary information for the use of the AHP and WLC methods. The combination of both methods, as a conditioning factor weighting mechanism for the generation of susceptibility maps was optimum for the study area.

Slope angle and geomorphology are the two factors that have the highest relative weight on instability. In the area, the presence of glacial deposits and steep slopes exposed to the sun are the predominant conditions in the generation of instability processes. The slopes showing high and very high (4 and 5) degrees of susceptibility are the slopes located to the west of the Upsala Channel (near the front of the Upsala Glacier), the slopes containing the Bertacchi and Cono Tributary Glaciers, and the slopes located over the Moyano and Norte Valleys. These slopes have a combination of conditioning factors that make the increase in susceptibility possible; they show slopes superior to 45° and are exposed to sunlight (orientated East-Northeast). Also, the lithology forming these slopes is vulcanite, highly fissile, and prone to fragmentation, and shows the presence of geological faults traversing these valleys. The final susceptibility map shows valuable information for the area, since, despite the fact that there are not any population facilities, touristic ships enter the area daily every summer season to appreciate the superb scenery. As final remarks, it is relevant to take into account the susceptibility to the instability processes in this area of the Los Glaciares National Park in order to prevent a possible hazard that may cause severe damages downstream and the ships that navigate the area. In addition, the results contribute to the decision-making of the organizations responsible for the reduction, prevention, and mitigation of the risks associated with these events in the North Branch of Argentino Lake.

Acknowledgements This research was funded by the Agencia Nacional de Ciencia y Tecnología de Argentina (PICTO 2016-0050) and for a scholarship provided by Centro Centro Latinoamericano de Formación Interdisciplinario (CELFI). Special thanks to the Instituto de Altos Estudios Espaciales Mario Gulich—Comisión Nacional de Actividades Espaciales (CONAE, Argentina) and authorities of the Los Glaciares National Park, Argentina. Also, we appreciate the collaboration of Marcelo Scavuzzo, Almendra Brasca Merlín, and Daniel Falaschi. This study is part of the PhD thesis of geographer Silvana Moragues.

References

Ahmed B (2015) Landslide susceptibility mapping using multi-criteria evaluation techniques in Chittagong metropolitan area, Bangladesh. Landslides 12(6):1077–1095

Ayalew L, Yamagishi H, Ugawa N (2004) Landslide susceptibility mapping using GIS-based weighted linear combination, the case in Tsugawa area of Agano river, Niigata prefecture, Japan. Landslides 1:73–81. https://doi.org/10.1007/s10346-003-0006-9

Ayalew L, Yamagishi H, Marui H, Kanno T (2005) Landslides in Sado Island of Japan: part II. GIS-based susceptibility mapping with comparisons of results from two methods and verifications. Eng Geol 81:432–445. https://doi.org/10.1016/j.enggeo.2005.08.004

Barredo JI, Benavides A, Hervas J, vanWesten CJ (2000) Comparing heuristic landslide hazard assessment techniques using GIS in the Tirajana basin, Gran Canaria Island, Spain. Int J Appl Earth Obs Geoinf 2(1):9–23. https://doi.org/10.1016/S0303-2434(00)85022-9

Basu T, Pal S (2017) Exploring landslide susceptible zones by analytic hierarchy process (AHP) for the Gish river basin, West Bengal. India Spat Inf Res 25(5):665–675. https://doi.org/10.1007/s41324-017-0134-2

Beigt D, Villarosa G, Outes V, Gómez EA, Toyos G (2019) Remobilized Cordón Caulle 2011 tephra deposits in north-Patagonian watersheds: resedimentation at deltaic environments and its implications. Geomorphology 34:140–152

Brabb E, Pampeyan H, Bonilla MG (1972) Landslide susceptibility in San Mateo County, California. U. S. Geological survey miscellaneous field studies map MF360, scale 1: 62,500

Carrasco J, Casassa G, Rivera A (2002) Meteorological and climatological aspects of the southern Patagonian ice fields the Patagonian ice fields. Springer, Boston MA

Chen W, Pourghasemi HR, Naghibi SA (2017) Prioritization of landslide conditioning factors and its spatial modeling in Shangnan County, China using GIS-based data mining algorithms. Bull Eng Geol Env. https://doi.org/10.1007/s10064-017-1004-9

Clarke BA, Burbank DW (2010) Bedrock fracturing, threshold hillslopes, and limits to the magnitude of bedrock landslides. Earth Planet Sci Lett 297(3–4):577–586. https://doi.org/10.1016/j.epsl.2010.07.011

Corominas J, Copons R, Villaplana JM, Altimir J, Amigó J (2003) Integrated landslide susceptibility analysis and hazard assessment in the principality of Andorra. Nat Hazards 30:421–435. https://doi.org/10.1023/B:NHAZ.0000007094.74878.d3

Corominas J, Van Westen C, Frattini P, Cascini L, Malet JP, Fotopoulou S, Catani F, Van Den Eeckhaut M, Mavrouli O, Agliardi F, Pitilakis K, Winter MG, Pastor M, Ferlisi S, Tofani V, Hervás J, Smith JT, Pitilakis K (2014) Recommendations for the quantitative analysis of landslide risk. Bull Eng Geol Env 73(2):209–263. https://doi.org/10.1007/s10064-013-0538-8

Cruden DM (1991) A simple definition of a landslide. Bull Int As Eng Geol 43:27–29. https://doi.org/10.1007/BF02590167

Cruden DM, Martin CD (2013) Assessing the stability of a natural slope. Global view of engineering geology and the environment. Taylor & Francis Group, London

Cubito A, Ferrara V, Pappalardo G (2005) Landslide hazard in the Nebrodi Mountains (Northeastern Sicily). Geomorphology 66:359–372. https://doi.org/10.1016/j.geomorph.2004.09.020

Dai FC, Lee CF (2001) Terrain-based mapping of landslide susceptibility using a geographical information system: a case study. Can Geotech J 38:911–923. https://doi.org/10.1139/t01-021

Eastman JR, Jin W, Kyem PAK, Toledano J (1995) Raster procedures for multi-criteria/multi-objetive decisions. Photogramm Eng Remote Sen 61:539–547

Ercanoglu M, Gokceoglu C (2002) Assessment of landslide susceptibility for a landslide-prone area (north of Yenice, NW Turkey) by fuzzy approach. Environ Geol 41(6):720–730. https://doi.org/10.1007/s00254-001-0454-2

Feizizadeh B, Blaschke T (2013) GIS-multicriteria decision analysis for landslide susceptibility mapping: comparing three methods for the Urmia lake basin. Iran Nat Hazard 65(3):2105–2128. https://doi.org/10.1007/s11069-012-0463-3

Feizizadeh B, Roodposhti MS, Jankowski P, Blaschke T (2014) A GIS-based extended fuzzy multi-criteria evaluation for landslide susceptibility mapping. Comput Geosci 73:208–221

Felicísimo AM (1994) Modelos digitales del terreno: introducción y aplicación en las ciencias ambientales. https://www.etsimo.uniovi.es/~feli

Fell R, Corominas J, Bonnard C, Cascini L, Leroi E, Savage WZ (2008) Guidelines for landslide susceptibility, hazard and risk zoning for land use planning. Eng Geol 102(3–4):85–98

Foresta L, Gourmelen N, Weissgerber F, Nienow P, Williams JJ, Shepherd A, Plummer S (2018) Heterogeneous and rapid ice loss over the Patagonian ice fields revealed by CryoSat-2 swath radar altimetry. Remote Sens Environ 211:441–455

Garreaud R, Lopez P, Minvielle M, Rojas M (2013) Large-scale control on the Patagonian climate. J Clim 26(1):215–230. https://doi.org/10.1175/JCLI-D-12-00001.1

Gerrard J (1994) The landslide hazard in the Himalayas: geological control and human action. Geomorphology and natural hazards. Elsevier, Amsterdam, pp 221–230

Ghiglione MC, Suarez F, Ambrosio A, Da Poian G, Cristallini EO, Pizzio MF, Reinoso RM (2009) Structure and evolution of the Austral basin fold-thrust belt, southern Patagonian Andes. Revista de la Asociación Geológica Argentina 65(1):215–226

Glasser NF, Jansson KN, Harrison S, Kleman J (2008) The glacial geomorphology and Pleistocene history of South America between 38°S and 56°S. Quatern Sci Rev 27:365–390

Glasser NF, Ghiglione MC (2009) Structural, tectonic and glaciological controls on the evolution of fjord landscapes. Geomorphology 105(3):291–302

Gorsevski PV, Jankowski P, Gessler PE (2006a) A heuristic approach for mapping landslide hazard by integrating fuzzy logic with analytic hierarchy process. Control Cybern 35(1):121–146

Gorsevski PV, Gessler PE, Boll J, Elliot WJ, Foltz RB (2006b) Spatially and temporally distributed modeling of landslide susceptibility. Geomorphology 80(3–4):178–198. https://doi.org/10.1016/j.geomorph.2006.02.011

Guzzetti F, Carrara A, Cardinali M, Reichenbach P (1999) Landslide hazard evaluation: an aid to a sustainable development. Geomorphology 31:181–216. https://doi.org/10.1016/S0169-555X(99)00078-1

Guzzetti F, Reichenbach P, Ardizzone F, Cardinali M, Galli M (2006) Estimating the quality of landslide susceptibility models. Geomorphology 81(1–2):166–184. https://doi.org/10.1016/j.geomorph.2006.04.007

Hasekiogullari GD, Ercanoglu M (2012) A new approach to use AHP in landslide susceptibility mapping: a case study at Yenice (Karabuk, NW Turkey). Nat Hazards 63(2):1157–1179. https://doi.org/10.1007/s11069-012-0218-1

Hervás J, Barredo JI, Rosin PL, Pasuto A, Mantovani F, Silvano S (2003) Monitoring landslides from optical remotely sensed imagery: the case history of Tessina landslide. Italy Geomorphol 54(1–2):63–75. https://doi.org/10.1016/S0169-555X(03)00056-4

Hung LQ, Van NT, Van Son P, Khanh NH, Binh LT (2016) Landslide susceptibility mapping by combining the analytical hierarchy process and weighted linear combination methods: a case study in the upper Lo river catchment (Vietnam). Landslides 13(5):1285–1301. https://doi.org/10.1007/s10346-015-0657-3

IUGS (1997) Working group on landslides, committee on risk assessment: quantitative risk assessment for slopes and landslides—the state of the art. In: Cruden D, Fell R (eds) Landslide risk assessment. Balkema, Rotterdam, pp 3–12

Jankowski P, Richard L (1994) Integration of GIS-based suitability analysis and multicriteria evaluation in a spatial decision support system for route selection. Environ Plan B: Plan Des 21(3):323–340. https://doi.org/10.1068/b210323

Kawabata D, Bandibas J (2009) Landslide susceptibility mapping using geological data, a DEM from ASTER images and an artificial neural network (ANN). Geomorphology 113(1–2):97–109. https://doi.org/10.1016/j.geomorph.2009.06.006

Kayastha P, Dhital MR, De Smedt F (2012) Landslide susceptibility mapping using the weight of evidence method in the Tinau watershed. Nepal Nat Hazards 63(2):479–498. https://doi.org/10.1007/s11069-012-0163-z

Kayastha P, Dhital MR, De Smedt F (2013) Application of the analytical hierarchy process (AHP) for landslide susceptibility mapping: a case study from the Tinau watershed, west Nepal. Comput Geosci 52:398–408. https://doi.org/10.1016/j.cageo.2012.11.003

Kraemer PE, Riccardi AC (1997) Estratigrafía de la región comprendida entre los lagos Argentino y Viedma (49° 40′–50° 10′ lat, S), Provincia de Santa Cruz. Revista de la Asociación Geológica Argentina 52(3):333–360

Ladas I, Fountoulis I, Mariolakos I (2007) Using GIS & multicriteria decision analysis in landslide susceptibility mapping—a case study in messinia prefecture area (Sw Peloponnesus, Greece). Bull Geol Soc Greece 40(4):13

Leir M, Michell A, Ramsay S (2004) Regional landslide hazard susceptibility mapping for pipelines in British Columbia. Geo-engineering for the society and its environment. 57th Canadian geotechnical conference and the 5th Joint CGS-IAH conference, 24–27 October, Old Quebec, Canada, 1–9

Lo Vecchio A, Lenzano MG, Richiano S, Lenzano LE (2016) Identificación y caracterización litológica mediante el uso del sensor ETM+ (Landsat 7). Caso de estudio: entorno del glaciar Upsala, Argentina. Revista de teledetección: Revista de la Asociación Española de Teledetección 46:57–72. https://doi.org/10.4995/raet.2016.4482

Marcano A, Cartaya S, Pacheco H, Méndez W (2015) Estimación de pesos ponderados de variables para generar mapas de susceptibilidad a movimientos en masa a través de la evaluación espacial multicriterios. Terra Nueva Etapa 31(50):55–80

Marinoni O (2004) Implementation of the analytical hierarchy process with VBA in ArcGIS. Comput Geosci 30:637–646. https://doi.org/10.1016/j.cageo.2004.03.010

Marta RT, Kerle N, Jetten V, van Western CJ, Kumar KV (2010) Characterising spectral, spatial and morphometric properties of landslides for semiautomatic detection using object-oriented methods. Geomorphology 116:24–36. https://doi.org/10.1016/j.geomorph.2009.10.004

McColl ST (2015) Landslide causes and triggers. Landslide hazards, risks and disasters. Academic Press, Cambridge, pp 17–42

Meena S, Mishra B, Tavakkoli Piralilou S (2019) A hybrid spatial multi-criteria evaluation method for mapping landslide susceptible areas in Kullu valley. Himalayas Geosci 9(4):1–18. https://doi.org/10.3390/geosciences9040156

Mondal S, Maiti R (2012) Landslide susceptibility analysis of Shiv-Khola watershed, Darjiling: a remote sensing & GIS based analytical hierarchy process (AHP). J Indian Soc Remote Sens 40(3):483–496. https://doi.org/10.1007/s12524-011-0160-9

Moragues S (2020) Estimación y evaluación de los procesos de inestabilidad de laderas mediante el uso de técnicas en sensoramiento remoto en el Brazo Norte del lago Argentino (Patagonia Austral, Argentina). Tesis de doctorado. Universidad Nacional de Río Negro, General Roca, Río Negro, Argentina. pp 230

Moragues S, Lenzano MG, Vecchio AL, Falaschi D, Lenzano L (2018) Surface velocities of Upsala glacier, southern Patagonian Andes, estimated using cross-correlation satellite imagery: 2013–2014 period. Andean Geol 45(1):87–103

Moragues S, Lenzano MG, Moreiras S, Lo Vecchio A, Lannutti E, Lenzano L (2019a) Slope instability analysis in South Patagonia applying multivariate and bivariate techniques on Landsat images during 2001–2015 period. CATENA 174:339–352. https://doi.org/10.1016/j.catena.2018.11.024

Moragues S, Lenzano MG, Moreiras S, Lenzano L (2019b) Paraglacial geomorphology associated with slope instability in the north branch of the Argentino Lake, Argentinean Patagonia. Cuadernos de Investigación Geográfica 45(1):367–392. https://doi.org/10.18172/cig.3786

Moreiras SM (2005) Landslide susceptibility zonation in the Río Mendoza Valley, Argentina. Geomorphology 66:345–357. https://doi.org/10.1016/j.geomorph.2004.09.019

Moreiras SM (2009) Análisis estadístico probabilístico de las variables que condicionan la inestabilidad de las laderas en los valles de los ríos Las Cuevas y Mendoza. Revista de la Asociación Geológica Argentina 65(4):780–790

Myronidis D, Papageorgiou C, Theophanous S (2016) Landslide susceptibility mapping based on landslide history and analytic hierarchy process (AHP). Nat Hazards 81(1):245–263. https://doi.org/10.1007/s11069-015-2075-1

Naruse R, Casassa G (1985) Reconnaissance survey of some glaciers in the southern Icefield. In: Nakajima C (ed) Glaciological studies in patagonia northern icefield, 1983–1984. Japanese Society of Snow and Ice, Data Center for Glacier Research, pp 121–133

Nefeslioglu HA, Duman TY, Durmaz S (2008) Landslide susceptibility mapping for a part of tectonic Kelkit valley (eastern black sea region of Turkey). Geomorphology 94(3–4):401–418. https://doi.org/10.1016/j.geomorph.2006.10.036

Palma Herrera JL (2015) Sistema de información geográfico (sig) y metodologías de evaluación multicriterio (EMC) en la búsqueda de escenarios alternativos para las áreas urbanas populares de la Ciudad de Comayagua. Revista Ciencias Espaciales 8(2):452–461

Pourghasemi HR, Pradhan B, Gokceoglu C (2012) Application of fuzzy logic and analytical hierarchy process (AHP) to landslide susceptibility mapping at Haraz watershed. Iran Nat hazards 63(2):965–996. https://doi.org/10.1007/s11069-012-0217-2

Qiao G, Lu P, Scaioni M, Xu S, Tong X, Feng T, Wu H, Chen W, Tian Y, Wang W, Li R (2013) Landslide investigation with remote sensing and sensor network: from susceptibility mapping and scaled-down simulation towards in situ sensor network design. Remote Sens 5:4319–4346. https://doi.org/10.3390/rs5094319

Rahim I, Ali SM, Aslam M (2018) GIS Based landslide susceptibility mapping with application of analytical hierarchy process in district Ghizer, Gilgit Baltistan Pakistan. J Geosci Environ Prot 6(02):34–49. https://doi.org/10.4236/gep.2018.62003

Razak KA, Santangelo M, Van Westen CJ, Straatsma MW, de Jong SM (2013) Generating an optimal DTM from airborne laser scanning data for landslide mapping in a tropical forest environment. Geomorphology 190:112–125. https://doi.org/10.1016/j.geomorph.2013.02.021

Regmi AD, Dhital MR, Zhang JQ, Su LJ, Chen XQ (2016) Landslide susceptibility assessment of the region affected by the 25 April 2015 Gorkha earthquake of Nepal. J Mater Sci 13:1941–1957

Roa JG (2007) Estimación de áreas susceptibles a deslizamientos mediante datos e imágenes satelitales: cuenca del río Mocotíes. Estado Mérida-Venezuela Revista Geográfica Venezolana 48(2):183–219

Saaty TL (1977) A scaling method for priorities in hierarchical structures. J Math Psychol 15:234–281. https://doi.org/10.1016/0022-2496(77)90033-5

Saaty TL (1980) The analytic hierarchy process: planning, priority setting, resource allocation. McGraw-Hill Book Co, New York, p 287
Saaty TL (2000) The fundamentals of decision making and priority theory with the analytic hierarchy process, 2nd edn. RWS Publications, Pitsburg, p 478
Saaty TL (2008) Decision making with the analytic hierarchy process. Int J Serv Sci 1(1):83–98
Saaty TL, Vargas LG (2001) Models, methods, concepts and applications of the analytic hierarchy process. Kluwer, Dordrecht, p 333
Sagredo EA, Lowell TV (2012) Climatology of Andean glaciers: a framework to understand glacier response to climate change. Glob Planet Chang 86:101–109. https://doi.org/10.1016/j.gloplacha.2012.02.010
Sakakibara D, Sugiyama S, Sawagaki T, Marinsek S, Skvarka P (2013) Rapid retreat, acceleration and thinning of Glaciar Upsala, southern Patagonia Icefield, initiated in 2008. Ann Glaciol 54(63):131–138
Scaioni M (2013) Remote sensing for landslide investigations: From research into practice. Remote Sens 5:5488–5492. https://doi.org/10.3390/rs5115488
Shahabi H, Hashim M (2015) Landslide susceptibility mapping using GIS-based statistical models and remote sensing data in tropical environment. Sci Rep. https://doi.org/10.1038/srep09899
Skvarca P, Satow K, Naruse R, Leiva J (1995) Recent thinning, retreat and flow of Upsala Glacier, Patagonia. Bull Glacier Res 13:11–20
Suárez J (2009) Deslizamientos volumen 1: análisis geotécnico. Primera edición, Bucaramanga
Thanth LN, De Smedt F (2012) Application of an analytical hierarchical process approach for landslide susceptibility mapping in a Luoi district, Thua Thien Hue province. Vietnam Environ Earth Sci 66:1739. https://doi.org/10.1007/s12665-011-1397-x
Tofelde S, Dusing W, Schildgen TF, Wittmann H, Alonso R, Strecker MR (2017) Changes in denudation rates and erosion processes in the transition from a low-relief, arid orogen interior to a high-relief, humid mountain-front setting, Toro basin, southern central Andes, American geophysical union, abstract, fall meeting
Varnes DJ (1984) International association of engineering geology commission on landslides and other mass movements on slopes landslide hazard zonation a review of principles and practice. Int As Eng Geol UNESCO Nat Hazard Ser 3:63
Voogd H (1983) Multi-criteria evaluations for urban and regional planning. Princeton University, London
Wu CH, Chen SC (2009) Determining landslide susceptibility in central Taiwan from rainfall and six site factors using the analytical hierarchy process method. Geomorphology 112:190–204
Yalcin A (2008) GIS-based landslide susceptibility mapping using analytical hierarchy process and bivariate statistics in Ardesen (Turkey): comparisons of results and confirmations. CATENA 72(1):1–12. https://doi.org/10.1016/j.catena.2007.01.003
Yan G, Liang S, Gui X, Xie Y, Zhao H (2018) Optimizing landslide susceptibility mapping in the Kongtong district, NW China: comparing the subdivision criteria of factors. Geocarto Int. https://doi.org/10.1080/10106049.2018.1499816
Yilmaz I, Yildirim M (2006) Structural and geomorphological aspects of the Kat landslides (Tokat-Turkey), and susceptibility mapping by means of GIS. Environ Geol 50(4):461–472. https://doi.org/10.1007/s00254-005-0107-y
Yoshimatsu H, Abe S (2006) A review of landslide hazards in Japan and assessment of their susceptibility using an analytical hierarchic process (AHP) method. Landslides 3(2):149–158
Zhu A, Wang R, Qiao J, Qin C, Chen Y, Liu J, Du F, Lin Y, Zhu T (2014) An expert knowledge-based approach to landslide susceptibility mapping using GIS and fuzzy logic. Geomorphology 214:128–138. https://doi.org/10.1016/j.geomorph.2014.02.003